Journal of Applied Polymer Science

Exploring Poly(vinyl alcohol) Hydrogels Containing Drug–Cyclodextrin Complexes as Controlled Drug Delivery Systems

Subhraseema Das, Usharani Subuddhi
Department of Chemistry, National Institute of Technology, Rourkela 769008, India
Correspondence to: U. Subuddhi (E-mail: subuddhiu@nitrkl.ac.in)

ABSTRACT: Poly(vinyl alcohol) (PVA) hydrogels containing drug–β-cyclodextrin inclusion complexes (ICs) were synthesized with glutaraldehyde (GA) as a crosslinker. The role of cyclodextrin (CD), the effect of the nature of drug, and the degree of crosslinking on the drug-release process were investigated. The probable mechanism of drug release was also explored. Controlled release of the drug was achieved from the hydrogels containing the ICs. The nature of the drug, in terms of its binding efficacy with CD, played an important role. The effect of the degree of crosslinking on the release pattern was strikingly different from that in the hydrogels containing free drug and those with ICs. The role of CD in the drug-release process was not only due to its inclusion ability but also its effect on the polymer relaxation. GA, apart from crosslinking PVA, probably interacted with the cyclodextrins and, thereby, influenced the matrix structure and the drug-release kinetics. © 2013 Wiley Periodicals, Inc. J. Appl. Polym. Sci. **2014**, *131*, 40318.

KEYWORDS: drug delivery systems; hydrophilic polymers; kinetics

Received 21 August 2013; accepted 14 December 2013
DOI: 10.1002/app.40318

INTRODUCTION

Since the report of the first hydrophilic gels by Wichterle and Lim,[1] hydrogels have found a wide spectrum of applications in pharmaceuticals, implants, biosensors, and drug-delivery systems. Hydrogels are hydrophilic polymers capable of imbibing large amounts of water or biological fluids.[2,3] They resemble the natural structure of the living tissues more than any other class of synthetic biomaterials because of their high water contents and soft consistency. Furthermore, the water content of these materials contributes to their biocompatibility.[4–7] Poly(vinyl alcohol) (PVA) is one of the most preferred starting materials for the synthesis of conventional hydrogels. The versatility of PVA is paramount in the fabrication of a variety of architectures, including hydrogels, microgels,[8,9] microspheres,[10–13] microbubbles,[14,15] and microcapsules.[16] Because of their good film-forming ability, long-term temperature, pH stability, and excellent biocompatibility, PVA hydrogels are much in demand in areas pertaining to biomedical research. Moreover, PVA is nontoxic, exhibits minimal cell adhesion and protein absorption, and has high oxygen- and aroma-barrier properties.[17] The pharmaceutical and biomedical utilities of PVA hydrogels are well documented.[18,19]

Pure PVA hydrogels are known to be very fragile in nature. Crosslinking and/or freeze–thawing methods are generally used to impart tougher mechanical properties to the hydrogel. PVA has been crosslinked by various physical and chemical processes, such as γ radiation,[20] photocrosslinking,[21] electron beam irradiation,[22] and reactions with bifunctional reagents such as epichlorohydrin, dialdehydes, acid chlorides, and dianhydrides.[23,24] However, the major drawback that is inevitably associated with PVA hydrogel is its inefficacy in controlling the initial burst release. For many medications, burst release has been known to cause patient noncompliance. Furthermore, burst release is a wasteful process because most of the drug released in this phase loses effectiveness both therapeutically and economically.[25] To substantiate PVA hydrogels as controlled drug-delivery devices, composite hydrogels have been designed as useful tools.[26,27] The incorporation of particulate systems (liposomes, micelles, etc.) into the hydrogel matrix has also been used to achieve a sustained drug-release profile.[28,29]

Cyclodextrin (CD) and its derivatives are of special interest in this context because of their hydrophilic exterior, which is useful for maintaining the bulk hydrophilicity and swelling state of the hydrogel and their hydrophobic interior. This can facilitate the entrapment and controlled release of a variety of drugs. Efforts are being made to incorporate CD into various polymer matrices to explore and modify current drug-release systems.[30,31] β-CD has been blended with PVA hydrogels, and it has been found that the presence of CD in the matrix prolonged the release of salicylic acid (SA).[32] Microspheres of PVA/CD have been synthesized and estimated for the inclusion and separation of drugs.[10] Functionalized β-cyclodextrin

(β-CD)-grafted PVA hydrogels also suggested the prolonged release of drugs.[33,34] Chemically modified PVA hydrogels containing methacrylated β-CD prepared by UV-induced polymerization have been studied for the sustained release of puerarin and acetazolamide.[35] PVA hydrogels containing α-cyclodextrin have also been prepared radiolytically.[36] However, the role of CD, the effect of nature of drug, and the effect of the degree of crosslinking on the drug-release process remains to be explored from systems involving PVA and CD.

In this study, glutaraldehyde (GA)-crosslinked PVA hydrogels were synthesized and preformed drug/β-CD inclusion complexes (ICs) were loaded into the polymer matrix. We judged the release behavior of the hydrogels by taking into account two drugs: the hydrophilic SA and the relatively hydrophobic ibuprofen (IBF). The synthesized hydrogels were characterized by Fourier transform infrared (FTIR) spectroscopy, X-ray diffraction (XRD), differential scanning calorimetry (DSC), and scanning electron microscopy (SEM) techniques. The swelling characteristics of the hydrogels were also evaluated. The drug-release profiles and the kinetic mechanisms were evaluated for both SA and IBF. The role of CD and the effects of the nature of the drug and the degree of crosslinking on the drug-release process were investigated.

EXPERIMENTAL

Materials

PVA having a molecular weight of 85,000–124,000 and degree of hydrolysis of 86–89% was purchased from S. D. Fine Chemical (India). IBF and β-CD were procured from Sigma-Aldrich (India). Analytical-reagent grade SA from Merck India, Ltd. was used. GA was obtained as a 25% w/w aqueous solution from Spectrochem Pvt., Ltd. (Mumbai, India). Triply distilled water was used throughout.

Preparation of the Solid Drug–β-CD IC

The solid IC of the drug and β-CD was prepared by the coprecipitation method.[37] Briefly, β-CD was dissolved in distilled water at 50°C in an oil bath for 1 h. The drug (SA or IBF) was solubilized in methanol and slowly added to the β-CD solution with constant stirring. The molar ratio of β-CD to drug was maintained at 1:1.2. The amount of drug used was in slight excess of the β-CD to ensure that all of the β-CD was complexed. The final solution was left undisturbed at room temperature for 3 days. The precipitated drug–β-CD IC was recovered by filtration and washed with methanol to remove the uncomplexed drug. The residue was vacuum-dried and used for further studies. A physical mixture (PM) of drug and β-CD was also prepared by the homogeneous blending of previously weighed 1:1 drug and β-CD in a mortar for 15 min.

Characterization of the Solid Drug–β-CD Complexes

FTIR Analysis. The FTIR spectra of β-CD, SA, IBF, the drug–β-CD ICs (SA–β-CD IC and IBF–β-CD IC), and the PMs (SA–β-CD PM and IBF–β-CD PM) were analyzed in a PerkinElmer RX I FTIR spectrophotometer. The samples were mixed with dry KBr and compressed into pellets and scanned from 4000 to 400 cm^{-1}.

XRD Studies. XRD profiles of the samples were collected on a PANalytical X-ray diffractometer with nickel-filtered Cu Kα radiation and scanned from 5 to 35° at room temperature at a scan rate of 3°/min.

Optical Microscopy. The morphologies of the samples were observed under a microscope (Olympus BX-51). The samples were placed on a glass slide, smeared with a cover slip, and then observed under the microscope.

DSC Studies. DSC was performed with a Mettler Toledo DSC822 instrument on 5–6-mg samples and scanned in perforated Al-pans under an N_2 atmosphere (purging rate = 40 mL/min) in the temperature range 50–200°C at a heating rate of 10°C/min.

^{1}H-NMR Studies. All of the NMR experiments were carried out in D_2O obtained from Sigma-Aldrich (India). Tetramethylsilane was used as a reference. The spectra were acquired on a Bruker 400-MHz NMR instrument at 298 K.

Hydrogel Preparation

PVA (10 wt %) was dissolved in water by heating at 80°C for 6 h. To the clear PVA solution, a desired amount of GA as a crosslinking agent and concentrated HCl as a catalyst were added, and the mixture was stirred at room temperature for an hour. To this mixture, a desired amount of drug or preformed drug–β-CD IC was added and stirred briefly at 200 rpm. The mixture was then poured into a clean and dried glass Petri dish of known surface area to obtain a film. The quantity of GA was varied to get a series of crosslinked hydrogels. GA-crosslinked PVA hydrogels and PVA hydrogels containing β-CD, in the absence of drug, were also synthesized and used for characterization and swelling studies (Table I).

The corresponding drug-loaded hydrogels were designated as P1-D, P2-D, P3-D, and P4-D for the PVA hydrogels having free drug, and the ones with the drug–β-CD ICs were designated P1C-D, P2C-D, P3C-D, and P4C-D.

Characterization of the Hydrogels

FTIR Analysis. The hydrogels were triturated with dry KBr, compressed to pellets, and scanned from 4000 to 400 cm^{-1} (64 average scans).

XRD Studies. XRD profiles of the hydrogels were recorded from 5 to 40° at room temperature at a scan rate of 3°/min.

Table I. Compositions of the Synthesized Hydrogels

Sample number	PVA (wt %)	β-CD (wt %)	GA (% v/v)	Sample designation
1	10	0	0.01	P1
2	10	0	0.02	P2
3	10	0	0.05	P3
4	10	0	0.1	P4
5	10	1	0.01	P1C
6	10	1	0.02	P2C
7	10	1	0.05	P3C
8	10	1	0.1	P4C

DSC Studies. DSC experiments were performed with a DSC Q200 V24.4 build 116 instrument. Dried hydrogel samples weighing around 3 mg were placed in aluminum crucibles, sealed with an Al lid, and then placed in a DSC instrument. The samples were first heated over the temperature range from 25 to 150°C (the first heating cycle) and then cooled to 25°C; this was followed by heating again up to 250°C (the second heating cycle), all at a heating rate of 10°C/min under nitrogen (purging rate = 40 mL/min). The reported results were taken from the second heating runs of the experiments to avoid experimental effects arising from the previous thermal history, structural relaxation, and incomplete chemical reactions.0

SEM. The morphologies of the hydrogels were observed with SEM (JEOL, model JSM 6480LV). The samples were swollen in a buffer solution of pH 7.4 until they reached equilibrium. They were then frozen at −80°C and lyophilized for 24 h with a LabTech freeze dryer. They were gold-coated *in vacuo* and mounted on metal stubs with double-sided adhesive tapes.

Equilibrium Swelling Measurement of the Hydrogels

The swelling characteristics of all of the prepared hydrogels was studied. The dried and preweighed samples were immersed in phosphate buffer solution (pH = 7.4) at 37°C until equilibrium swelling was achieved. They were taken out at regular intervals, and their weights were measured after they were gently wiped with tissue paper to remove excess surface water. The degree of swelling was calculated as follows:

$$\text{Degree of swelling}\,(\%) = \frac{W_s - W_d}{W_d} \times 100$$

where W_s and W_d are the weights of the swollen and dried hydrogels, respectively. The data were expressed as the mean values of three independent experiments, and the standard deviations are also presented as error bars.

In Vitro Release Studies

In vitro drug release was carried out after the immersion of the drug-loaded hydrogels into 50 mL of phosphate buffer (pH 7.4) at 37°C under constant stirring. We determined the quantity of drug released by monitoring the absorbance at 296 nm for SA and 276 nm for IBF in a Shimadzu ultraviolet–visible spectrophotometer (UV-1800) and taking out aliquots of 3 mL at particular time intervals. The withdrawn samples were replenished with fresh 3 mL of buffer to simulate physiological conditions. We estimated the amount of drug released by comparing the absorbance with the standard curves of the respective drugs. The release data were expressed as the mean values of three independent experiments, and the standard deviations are also presented as error bars.

Drug-Release Kinetics

To have an idea about the probable mechanism of drug release from the hydrogels, the release data were analyzed according to four basic kinetic models. These models are valid for the initial 60% of drug release. The data were analyzed with OriginPro 7 (OriginLab Corp.).

Model 1 is based on the Higuchi equation that describes the Fickian diffusion of a drug:[38]

$$M_t/M_\infty = kt^{0.5} \quad (1)$$

where M_t/M_∞ is the fractional drug release at time t and k is the Fickian diffusion kinetic constant.

Model 2 is described by the Ritger–Peppas equation:[39]

$$M_t/M_\infty = k't^n \quad (2)$$

where k' is the kinetic constant for the Ritger–Peppas equation, t is the release time, and n is the diffusional exponent that explains the drug-transport mechanism. When $n = 0.5$, the drug-release mechanism is Fickian diffusion, which occurs because of the molecular diffusion of the drug. When $n = 1$, case II transport occurs; this is associated with the relaxational release of the drug, which leads to zero-order kinetics. When n lies between 0.5 and 1, anomalous transport is observed, where both Fickian and relaxational phenomena contribute to the drug release. A value of $n > 1$ implies super case II transport mechanism, which is due to a large increase in osmotic pressure driving forces, followed by the relaxation and swelling of polymers.

Model 3 is based on the Peppas–Sahlin equation, and this accounts for the coupled effects of Fickian diffusion and case II transport:[40]

$$M_t/M_\infty = k_1 t^m + k_2 t^{2m} \quad (3)$$

The first term on the right-hand side of eq. (3) represents the contribution of Fickian diffusion (F), and the second term refers to the macromolecular relaxation contribution (R) to the overall release mechanism. k_1 is the diffusion kinetic constant, and k_2 is the relaxation rate constant. The coefficient m is the Fickian diffusional exponent, which depends on the geometry of the device. For thin films, the value of m is taken as 0.5.

With the estimated values of k_1 and k_2 obtained from the fitting of the experimental data to eq. (3), the ratio of R to F was calculated with eq. (4) as follows:

$$R/F = (k_2/k_1)t^m \quad (4)$$

Model 5 is the zero-order drug-delivery kinetics equation given as follows:

$$M_t/M_\infty = k''t \quad (5)$$

where k'' represents the zero-order kinetic rate constant.

Cytotoxicity Assay

Cytotoxicity assay of the prepared hydrogels was performed with 5-mm-diameter discs of the hydrogel films. The hydrogels were sterilized at a 15 lb/in.^{2} steam pressure at 121°C for 1 h and used for the cytotoxicity assay with the L-929 NCCS fibroblast cell line. Cell growth was performed on a 24-well tissue culture plate in a controlled atmosphere (5% CO_2 at 37°C) with Dulbecco's Modified Eagle's Medium (Hi-Media, India) cell culture medium supplemented with 10% fetal bovine serum (Hi-Media, India) and penicillin–streptomycin antibiotic solution (Hi-Media, India). Ninety percent confluent monolayers of cultured cells were harvested by trypsinization (0.25% trypsin and 0.02% ethylene diamine tetraacetic acid, Hi-Media, India), and 1 mL of 1×10^5 cells/mL was seeded in each well. The culture plate was then incubated for 48 h in a CO_2 incubator at

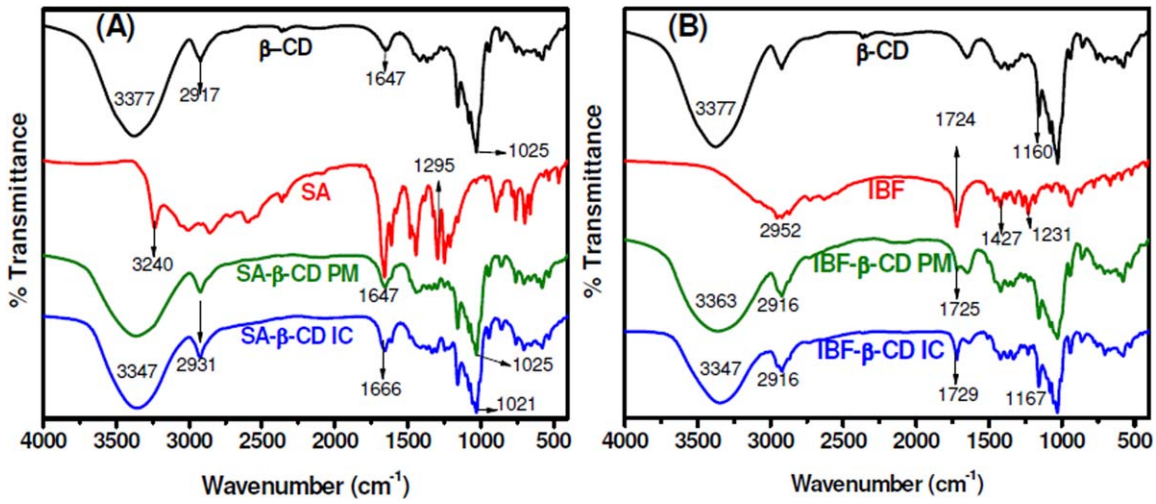

Figure 1. FTIR spectra of (A) *β*-CD, SA, SA–*β*-CD PM, and SA–*β*-CD IC and (B) *β*-CD, IBF, IBF–*β*-CD PM, and IBF–*β*-CD IC. [Color figure can be viewed in the online issue, which is available at wileyonlinelibrary.com.]

37°C. The cytotoxicity analysis was performed through MTT [3-(4,5-dimethylthiazol-2-yl)-2,5-diphenyltetrazolium bromide] assay as per standard protocol.[41]

RESULTS AND DISCUSSION

Characterization of the Drug–*β*-CD Solid ICs

FTIR Analysis. The FTIR spectrum of *β*-CD (Figure 1) shows the characteristic CD peaks, which included the broad band with a maximum at 3377 cm^{-1} due to the stretching vibrations of the hydroxyl groups, an absorption band at 2917 cm^{-1} attributed to C—H stretching, a band at 1647 cm^{-1} assigned to the bending vibrations of the O—H bonds in COH groups and/or in water molecules and a band at 1412 cm^{-1} due to the bending vibration of the C—H bonds in CH_2OH and CHOH groups.[42,43]

SA. The FTIR spectrum of SA [Figure 1(A)] presents bands attributed to the phenyl O—H stretching vibrations at 3240 cm^{-1}, C—H bending vibrations of aromatic protons at 1295 cm^{-1}, stretching of C═O bonds at 1647 cm^{-1}, and C═C bonds of benzene rings (1607, 1439, and 1495 cm^{-1}). The FTIR spectrum of the SA–*β*-CD PM was similar to that of *β*-CD. However, major shifts occurred in the spectrum of the SA–*β*–CD IC. Shifts in the absorption of the hydroxyl group to 3347 cm^{-1} and the carbonyl group to 1666 cm^{-1} were witnessed. These changes suggested the inclusion of the benzene ring of SA into the CD cavity.[44]

IBF. The FTIR spectrum of IBF [Figure 1(B)] shows the presence of a band at 1724 cm^{-1} corresponding to carbonyl stretching. Two bands arising from C═O stretching and O—H bending appeared in the spectrum at 1427 and 1231 cm^{-1}. A shift in the higher frequency of the characteristic acid carbonyl stretching in the IBF–*β*-CD IC to 1729 cm^{-1} was observed. This spectral shift indicated the inclusion of IBF into the *β*-CD cavity.[45,46]

XRD Studies. The formation of IC was indicated by the appearance of new or modified peaks from the original XRD

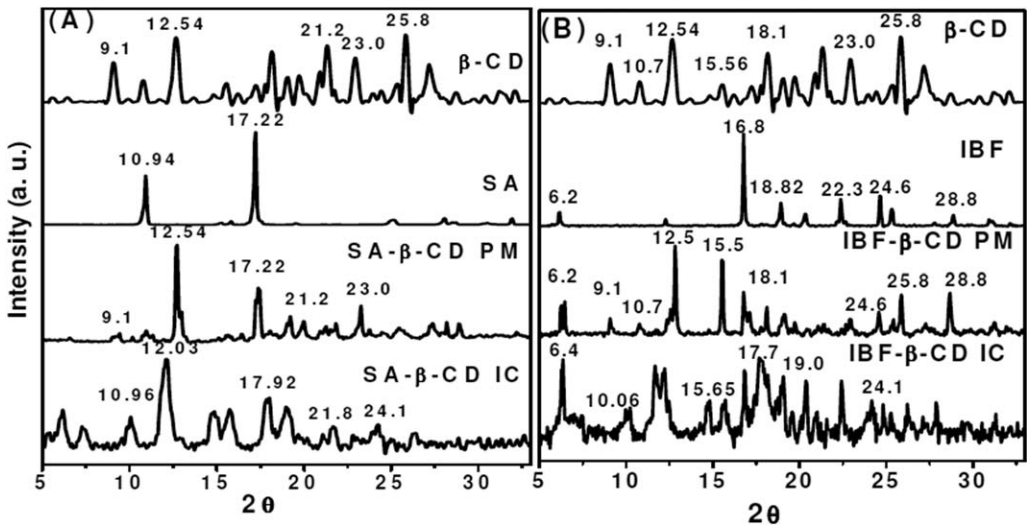

Figure 2. XRD profiles of (A) *β*-CD, SA, SA–*β*-CD PM, and SA–*β*-CD IC and (B) *β*-CD, IBF, IBF–*β*-CD PM, and IBF–*β*-CD IC.

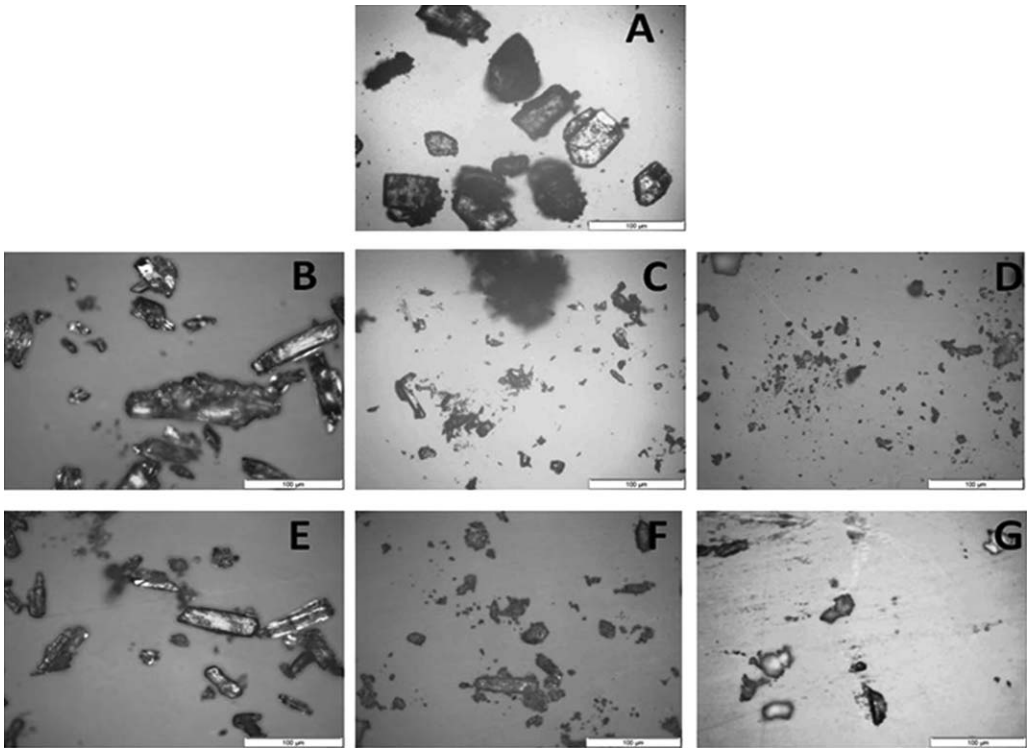

Figure 3. Optical microscopy images of (A) β-CD, (B) SA, (C) SA–β-CD PM, (D) SA–β-CD IC, (E) IBF, (F) IBF–β-CD PM, and (G) IBF–β-CD IC.

patterns.[47] The XRD profile of β-CD (Figure 2) included peaks at 9.1° (101), 12.54° (111), and 21.2° (410), and this suggested that β-CD adopted a cage-type structure.[48]

SA. The XRD profile of SA [Figure 2(A)] was composed of two sharp peaks at 10.94 and 17.22°, which indicated its crystalline nature. The PM (SA–β-CD PM) represented a superposition of the XRD patterns of individual components. However, in the XRD profile of the SA–β-CD IC, the shift in peak positions to 10.04, 12.03, 17.92, and 21.9° were observed; this suggested the formation of new phases that were probably due to the inclusion of SA into the β-CD cavity.[44,49]

IBF. The powder XRD profile of IBF [Figure 2(B)] exhibited numerous distinct peaks at 6.2, 12.14, 16.8, 18.82, 20.31, 22.37, and 24.6° that clearly pointed toward the crystalline nature of the drug. Principal peaks from IBF and β-CD were present in the IBF–β-CD PM. The diffraction profile of the IBF–β-CD IC presented a completely different pattern, with new peaks at 6.4, 10.06, and 17.7°, which indicated the formation of the IC.[37]

Optical Microscopy. The morphologies of the CD, drugs, PMs, and ICs were visualized by optical microscopy. The images of CD [Figure 3(A)], SA [Figure 3(B)], and IBF [Figure 3(E)] indicated their crystalline nature. The photographs of the PMs, SA–β-CD PM [Figure 3(C)], and IBF–β-CD PM [Figure 3(F)] showed both drug and CD crystals. However, the ICs pointed toward the formation of new entities.

DSC Studies. Figure 4 presents the DSC traces of the β-CD, SA–β-CD PM, SA–β-CD IC, IBF–β-CD PM, and IBF–β-CD IC. The thermogram of β-CD exhibited a broad endotherm around 130°C because of the dehydration process. The characteristic melting endotherms of IBF and SA have been reported at 76.3 and 158°C.[37,50] In the endotherm of the SA–β-CD PM, the dehydration endotherm from β-CD, and the melting endotherm from free SA were observed. On the contrary, the endotherm of the SA–β-CD IC presented a shift in the β-CD endotherm and lacked the characteristic drug endotherm. Thus, the DSC studies suggested an inclusion phenomenon of SA in β-CD. Similarly, the IBF–β-CD PM exhibited the endotherms of both β-CD and free IBF. The absence of the IBF endotherm in the IBF–β-CD

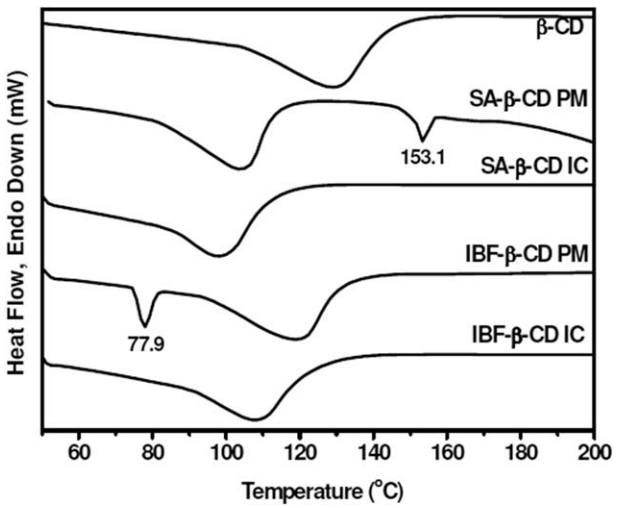

Figure 4. DSC thermograms of β-CD, SA–β-CD PM, SA–β-CD IC, IBF–β-CD PM, and IBF–β-CD IC.

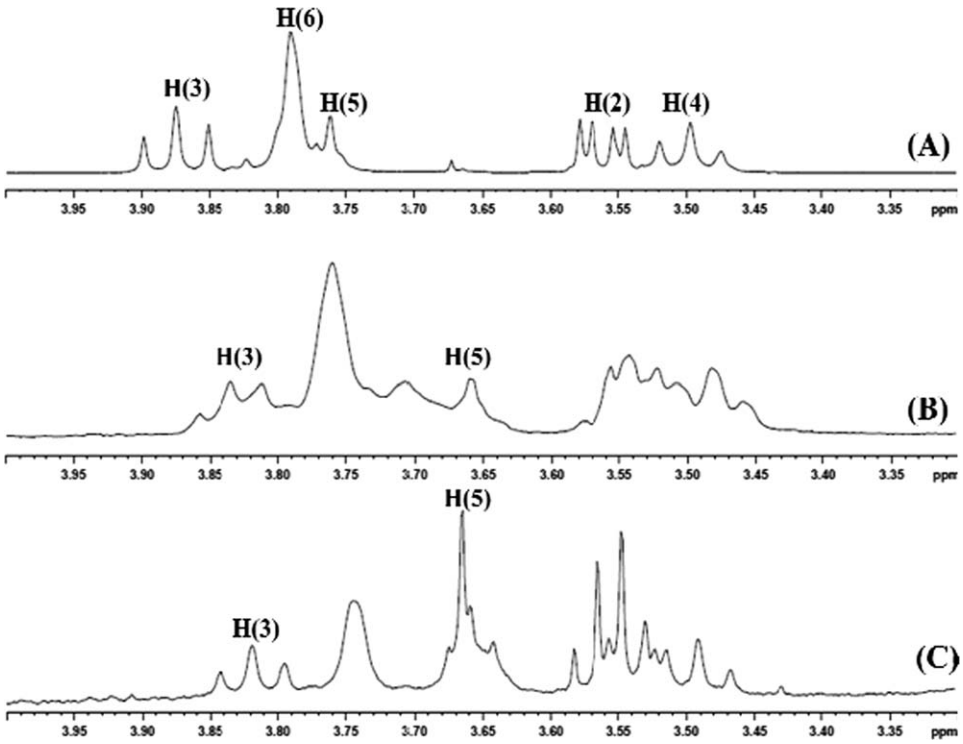

Figure 5. ^{1}H-NMR spectra of (A) β-CD, (B) SA–β-CD IC, and (C) IBF–β-CD IC in D_2O at 25°C.

IC and the shift of the β-CD endothermic transition to a lower temperature range indicated the complex formation.

^{1}H-NMR Studies. Direct evidence for the formation of the drug–β-CD IC could be obtained from ^{1}H-NMR. It is well known that β-CD has the topology of a hollow cone, with H-3 and H-5 being the inner protons. The hydrophobic guests get included in the toroidal cavity of β-CD and, thereby, affect the inner protons of the macrocycle.[37] The change in the chemical shifts in the H-3 [$\Delta(\delta H3)$] and H-5 [$\Delta(\delta H5)$] protons suggests the inclusion process. When $\Delta\delta H3 > \Delta\delta H5$, the inclusion of the guest inside the cavity is partial, whereas $\Delta(\delta H3) \leq \Delta(\delta H5)$ indicates total inclusion of the guest inside the β-CD cavity.[51]

The ^{1}H-NMR spectra of the β-CD, SA–β-CD IC, and IBF–β-CD IC are shown in Figure 5, and the chemical shifts (δs) of the β-CD protons are listed in Table II.

Table II. δ Values for the β-CD, SA–β-CD IC, and IBF–β-CD IC

	δ (ppm)		
	β-CD	SA–β-CD IC	IBF–β-CD IC
H-1	4.991	5.012	5.015
H-2	3.561	3.532	3.563
H-3	3.874	3.813	3.818
H-4	3.496	3.471	3.522
H-5	3.761	3.660	3.676
H-6	3.790	3.760	3.744

From Table II, it is noteworthy that the H-3 and H-5 protons shifted about 0.061 and 0.101 ppm, respectively, in SA–β-CD IC and 0.056 and 0.085 ppm, respectively, in IBF–β-CD IC with respect to the native β-CD. This clearly indicated that the drugs were totally included in the β-CD cavity.

Characterization of the Hydrogels

FTIR Analysis. Figure 6(A) presents the FTIR spectra of the P1 (PVA hydrogel with 0.01% GA) and P1C (PVA-CD hydrogel with 0.01% GA) hydrogels. The FTIR spectrum of the P1 hydrogel showed all of the characteristic peaks of PVA. A large band around 3400 cm^{-1} was due to O—H stretching. The C—H stretching from the alkyl group regions was observed around 2935 cm^{-1}, and the peak at 1720 cm^{-1} was attributed to the C═O stretching. The peak at 1140 cm^{-1} was attributed to the crystalline C═O stretching due to the semicrystalline nature of PVA. The FTIR spectrum of the P1C hydrogel showed the characteristic O—H and C—H peaks. However, the carbonyl stretching was modified, and the crystalline C═O peak was considerably reduced; this indicated a reduction in the crystallinity of the hydrogel upon incorporation of β-CD. Figure 6(B,C) displays the FTIR spectra of the P1, P2, P3, and P4 and P1C, P2C, P3C, and P4C hydrogels. It was evident that as crosslinking increased, there was a reduction in the crystalline nature of the hydrogels.

XRD Studies. Figure 7(A) illustrates the wide-angle XRD traces of the P1, P2, P3, and P4, and Figure 7(B) shows those of the P1C, P2C, P3C, and P4C hydrogels. The PVA hydrogel with the lowest GA content (P1) showed a peak around a diffraction angle (2θ) of 19.72° similar to that of pure PVA, which was

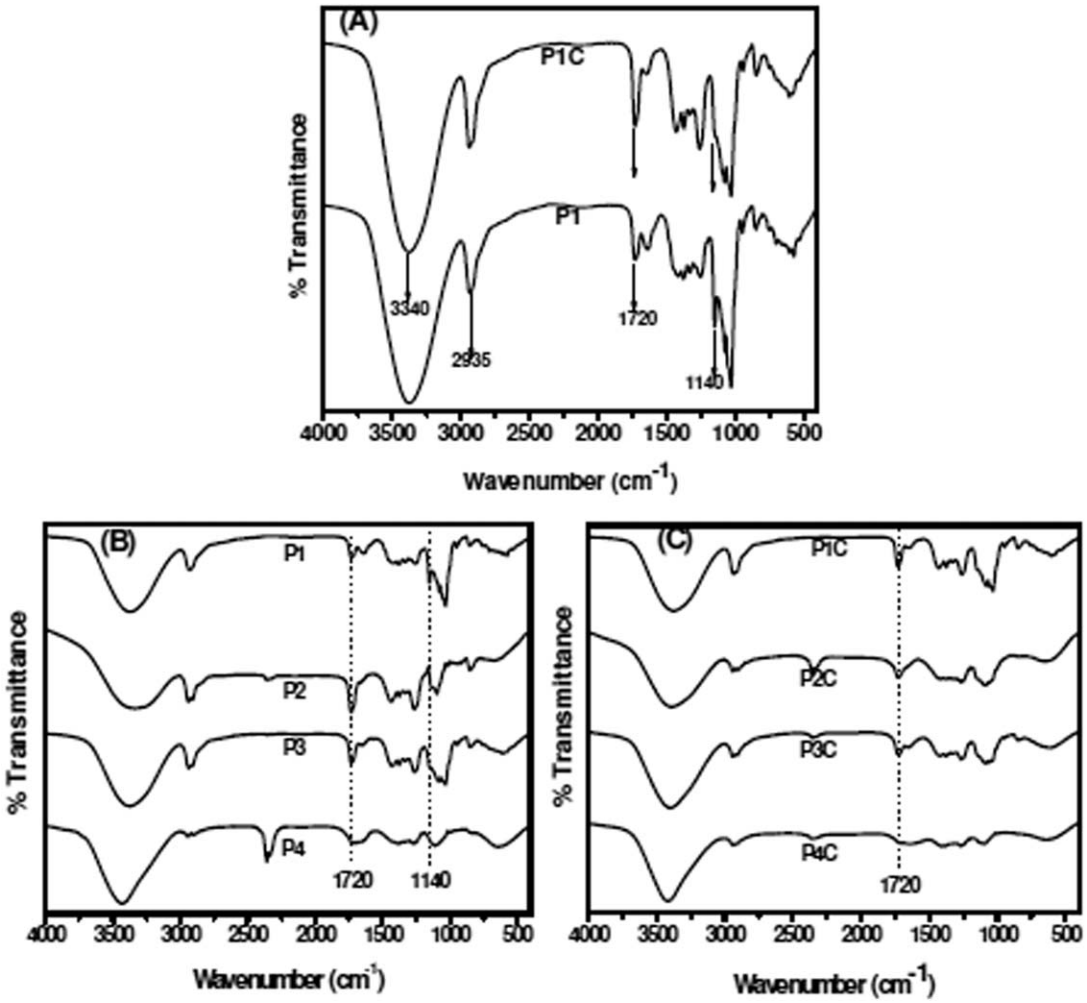

Figure 6. FTIR spectra of the (A) P1 and P1C, (B) P1, P2, P3, and P4 and (C) P1C, P2C, P3C, and P4C hydrogels.

associated with the crystalline phase of PVA, PVA being a semi-crystalline polymer. The decrease in the peak intensity in the case of the P1C hydrogel indicated a decrease in crystallinity in the sample; this was also supported by the FTIR data. This implied that in the presence of β-CD, the PVA chains were somewhat prevented from self-associating and crystallizing. This might have been because of the hydrogen-bonding interactions between the β-CD units and the PVA polymer chains. With

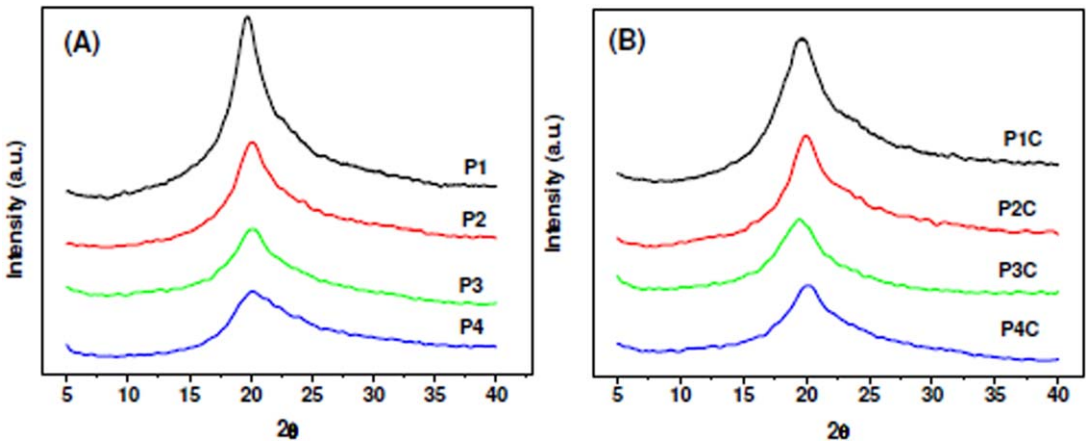

Figure 7. XRD profiles of the (A) P1, P2, P3, and P4 and (B) P1C, P2C, P3C, and P4C hydrogels. [Color figure can be viewed in the online issue, which is available at wileyonlinelibrary.com.]

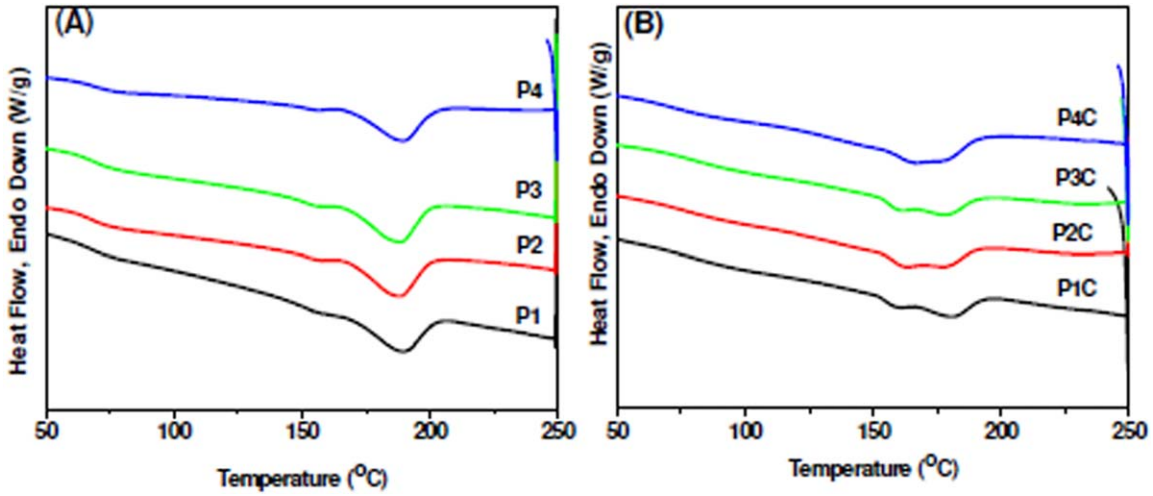

Figure 8. DSC thermograms of the (A) P1, P2, P3, and P4 and (B) P1C, P2C, P3C, and P4C hydrogels. [Color figure can be viewed in the online issue, which is available at wileyonlinelibrary.com.]

increasing GA content, there was a remarkable decrease in the crystalline reflection from PVA [Figure 7(A)]. It has been well established that GA disrupted the crystalline phase of PVA.[52] A similar effect was also observed for the P4C hydrogels [Figure 7(B)]. These samples showed a broad diffraction pattern typical of the amorphous phase. Hence, we concluded from the FTIR spectroscopy and XRD data that a higher content of GA and β-CD prevented the self-association of the PVA chains; this rendered a somewhat amorphous nature to the otherwise semicrystalline PVA matrix.

DSC Studies. Figure 8(A) represents the DSC thermograms of the P1, P2, P3, and P4 hydrogels. In the thermograms, the glass-transition temperature (T_g) and melting temperature (T_m) are clearly seen. T_g was found to decrease with increasing percentage of GA ($T_g \approx 68.7$°C for P1, $T_g \approx 67.5$°C for P2, $T_g \approx 67.2$°C for P3 and $T_g \approx 65.8$°C for P4); this implied that the increased crosslinking density resulted in a limited mobility of the polymer chains.[53] The melting enthalpy decreased with increasing GA content (Table III). This property was related to the membrane crystallinity. The addition of GA to the polymer increased the distance between the chains, and this made the organization of PVA in crystalline lattices difficult and resulted in the decrease in the melting enthalpy.[53] This was also clear from the decreased degree of crystallinity (X) with increasing crosslinking. X of the hydrogels was calculated from the given equation:

$$X = \frac{\Delta H}{\Delta H_c}$$

where ΔH is the heat of melting of the PVA sample and ΔH_c is the heat of melting of the 100% crystalline PVA, which is 138.60 J/g.[54,55]

Figure 8(B) represents the DSC thermograms of the P1C, P2C, P3C, and P4C hydrogels. They showed lower T_m's compared to the those of the corresponding hydrogels without β-CD, that is, P1, P2, P3, and P4 (Table III). This could have been due to the decreased crystallinity of the PVA matrix in the presence of β-CD, as was evident from the X values. For a given percentage of GA, the X value of the PVA matrix without β-CD was relatively higher than that of the corresponding hydrogel with β-CD. The T_m values of these hydrogels were also found to decrease with increasing GA content. This could have also been due to the restricted mobility of the chains due to the combined effect of CD and the increased matrix density due to crosslinking.

Table III. T_m, Enthalpy, and X Values of the Hydrogels

Sample	T_m (°C)	ΔH (J/g)	X (%)
P1	189.55	26.88	19.4
P2	187.75	24.68	17.8
P3	187.31	24.34	17.6
P4	187.11	24.11	15.6
P1C	181.00	25.77	18.6
P2C	177.90	24.15	17.4
P3C	177.79	22.17	16.0
P4C	177.45	19.59	14.3

SEM Analysis. The SEM micrographs (Figure 9) revealed the morphological dependence of the synthesized hydrogels on the extent of crosslinking. As the concentration of the crosslinker (GA) was increased, a distinct difference in the morphology of the hydrogels was observed. The P1and P2 hydrogels exhibited highly porous network structures with a spongy appearance. The morphology of P3 was more of a fibrillar kind. However, the matrix structure tightened upon the addition of 0.1% GA. As evident, the P4 hydrogel was relatively denser and compact with respect to others. Similar morphological behavior was observed for the P1C, P2C, P3C, and P4C hydrogels. The P1C and P2C hydrogels appeared to be porous, whereas the P3C hydrogel was observed to be somewhat fibrillar. The P4C hydrogel was found to be compact in nature, similar to that of the P4 hydrogel. Thus, we inferred that incorporation of β-CD did not affect the morphology of the PVA hydrogels.

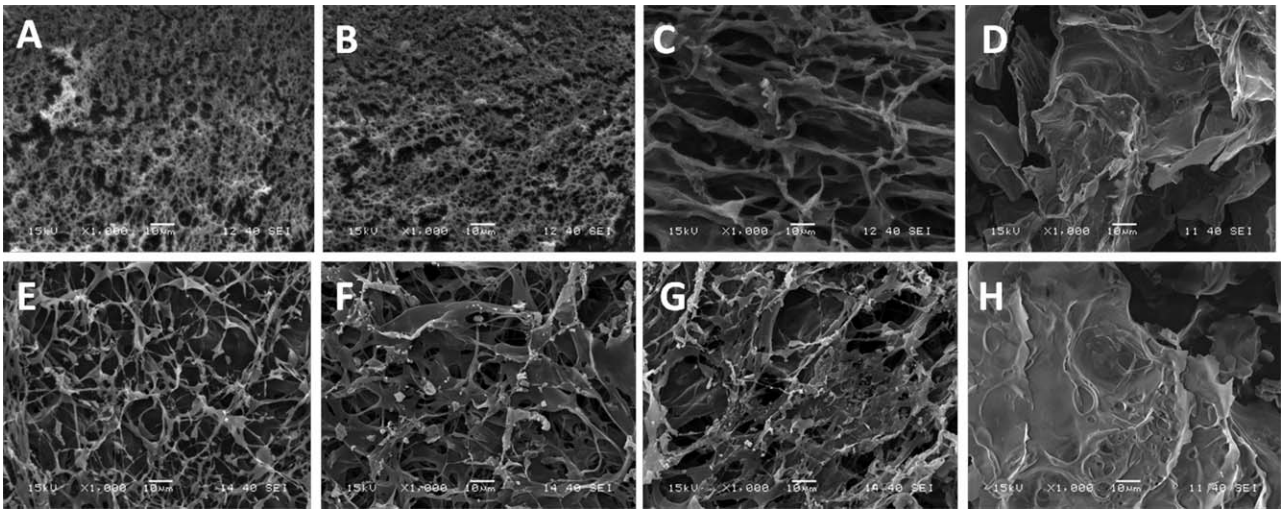

Figure 9. SEM micrographs of the (A) P1, (B) P2, (C) P3, (D) P4, (E) P1C, (F) P2C, (G) P3C, and (H) P4C hydrogels.

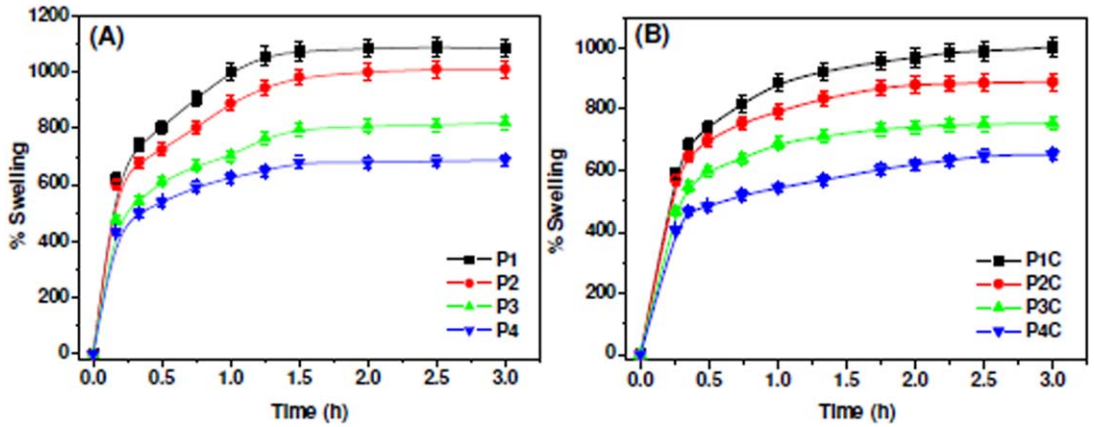

Figure 10. Swelling behavior of the hydrogels at pH 7.4 and 37°C: (A) P1, P2, P3, and P4 and (B) P1C, P2C, P3C, and P4C hydrogels. [Color figure can be viewed in the online issue, which is available at wileyonlinelibrary.com.]

Equilibrium Swelling Studies

Figure 10(A) shows that the equilibrium swelling of P1, P2, P3, and P4, and Figure 10(B) shows that of the P1C, P2C, P3C, and P4C hydrogels. With increasing crosslinker percentage, there was a gradual decrease in the degree of swelling observed for both types of hydrogels. This could be rationalized by the morphological dependence of these hydrogels on the crosslinker concentration. As evident from the SEM studies, the hydrogels with lower degrees of crosslinking were porous in nature and, therefore, could accommodate more water in their capillary pores. This resulted in a higher swelling ability. The decrease in swelling with increased crosslinker concentration could have been due to the increased matrix density, and this restricted the inward flow of solvent molecules.[56]

For a given crosslinker concentration, the swellability of the pure PVA hydrogel was relatively higher than that of the PVA hydrogels containing β-CD. This might have been to the formation of a slightly rigid hydrogel matrix upon the incorporation of CD because of the hydrogen-bonding interaction between the β-CD and PVA or the β-CD getting crosslinked to some extent in the presence of GA.

In vitro Drug-Release Studies

Drug Release from the Hydrogels. Figure 11(A) shows the drug-release profiles of SA from the P4-D and P4C-D hydrogels. As evident, the release patterns differed significantly from the two hydrogel matrices. The P4-D film showed an almost burst-type release of drug, and total drug release was observed in a short period. The presence of β-CD significantly prolonged the release of SA and showed a sustained release pattern from the P4C-D hydrogel. In the P4-D hydrogel, the drug was freely dispersed in the polymer matrix, and the drug, being a small molecule, easily diffused to the releasing medium as the hydrogel swelled. On the other hand, the P4C-D hydrogel contained the drug in the form of the IC with β-CD. For the drug-release process to be accomplished from the P4C-D hydrogel, the bound SA had to first be released into the polymer matrix, followed by the diffusion of the free drug from the matrix. Thus, the difference in the release rates observed between the previous

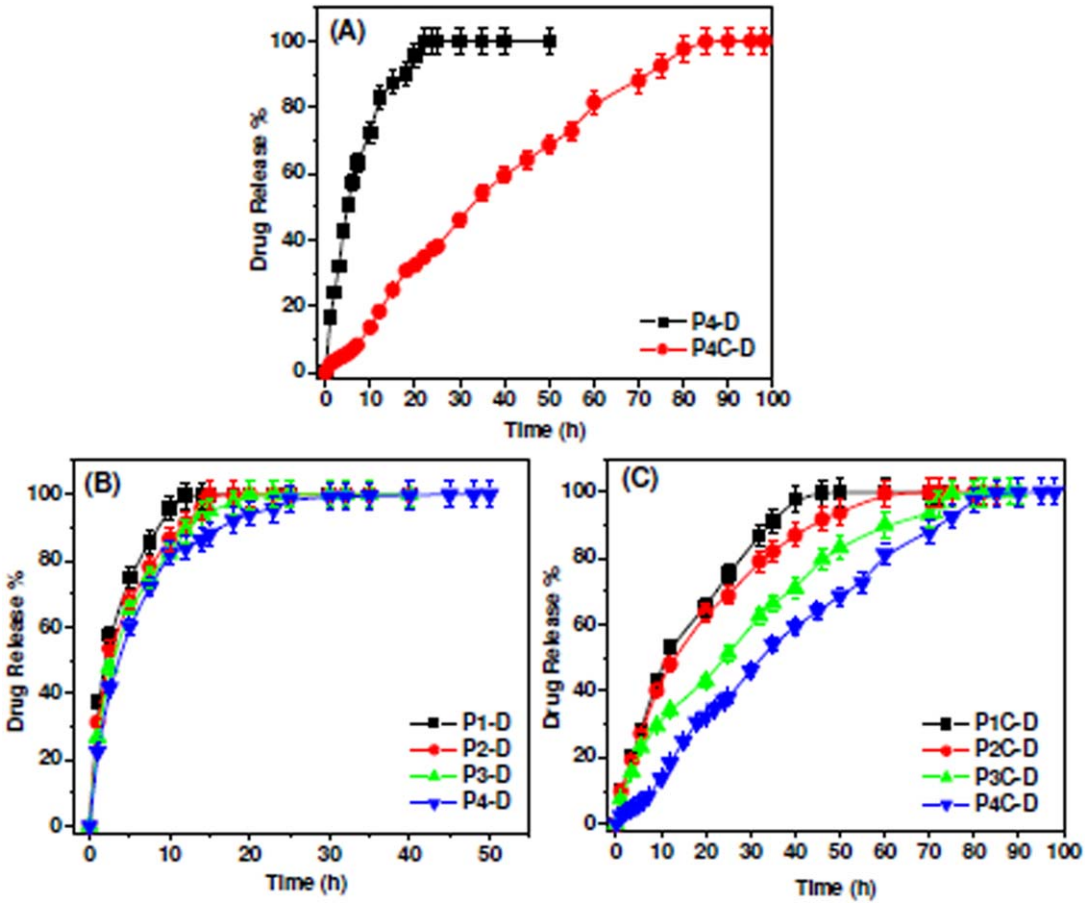

Figure 11. SA release profiles of the (A) P4-D and P4C-D, (B) P1-D, P2-D, P3-D, and P4-D, and (C) P1C-D, P2C-D, P3C-D, and P4C-D hydrogels. [Color figure can be viewed in the online issue, which is available at wileyonlinelibrary.com.]

two hydrogels was attributed to the diffusion barrier imposed by β-CD in terms of the inclusion process. This resulted in a slow release of the drug from the β-CD-containing hydrogel. However, it is known that even with the simple blending of β-CD with PVA, it is possible to achieve prolonged release of drug.[32] To verify whether the inclusion properties of β-CD were solely responsible for the slow release of the drug from the hydrogels, drug-release studies were carried out from the PVA hydrogels with the same β-CD and drug contents but with various crosslinker concentrations (the P1C-D, P2C-D, P3C-D, and P4C-D hydrogels). The release studies of the PVA hydrogels in the absence of β-CD at various crosslinker concentrations (the P1-D, P2-D, P3-D, and P4-D hydrogels) were also carried out for comparison.

Figure 11(B) depicts the SA release profiles of the P1-D, P2-D, P3-D, and P4-D hydrogels, and Figure 11(C) shows those of the PVA hydrogels containing the SA–β-CD IC (the P1C-D, P2C-D, P3C-D, and P4C-D hydrogels). As is evident in the figures, there was a striking difference in the release patterns as the GA concentration was varied. The drug-release profiles from the hydrogels containing the SA–β-CD ICs showed a strong dependence on the degree of crosslinking. With increasing GA concentration, the drug release was found to be considerably slower. On the other hand, for the hydrogels containing free drug, the effect of the GA concentration on the release rate was almost insignificant, and there was only a slight decrease in the release rate with increasing GA concentration. The release of the drug from any hydrogel is governed by various factors, such as hydrogel swelling, diffusion of the drug from the swollen matrix, and polymer relaxation. Therefore, any change in the hydrogel that affects the previous factors can influence the drug-release process. If hydrogel swelling and drug diffusion from the swollen matrix were the governing factors, both types of hydrogels would be expected to show similar release patterns with respect to the various crosslinker concentrations because they exhibited similar swelling behaviors with increasing GA percentage. Thus, the observed difference in the release patterns from these hydrogels with changes in the GA concentration could be rationalized only when the presence of β-CD was somehow influencing the polymer relaxation; this, in turn, affected the drug-release rate. Apart from crosslinking PVA, GA probably interacted with the hydroxyl groups of the β-CDs and further crosslinked the matrix. Thus, with increasing GA concentration, more and more β-CDs got crosslinked. As a result, the polymer matrix was modified, and the drug-release rate was reduced. Among all of the hydrogels studied, P4C-D was found to show the

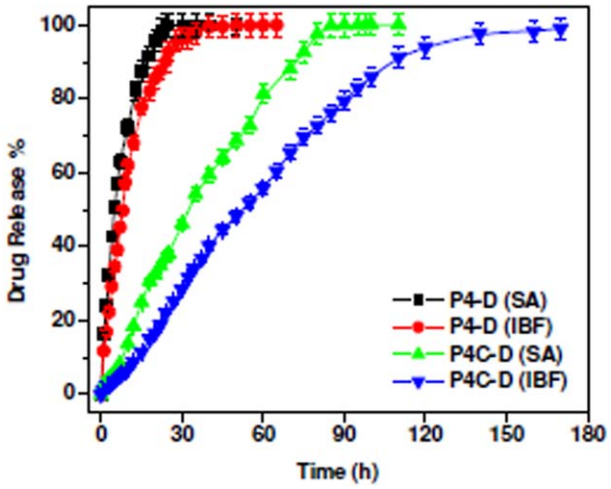

Figure 12. Comparison of the release profiles of SA and IBF from the P4-D and P4C-D hydrogels. [Color figure can be viewed in the online issue, which is available at wileyonlinelibrary.com.]

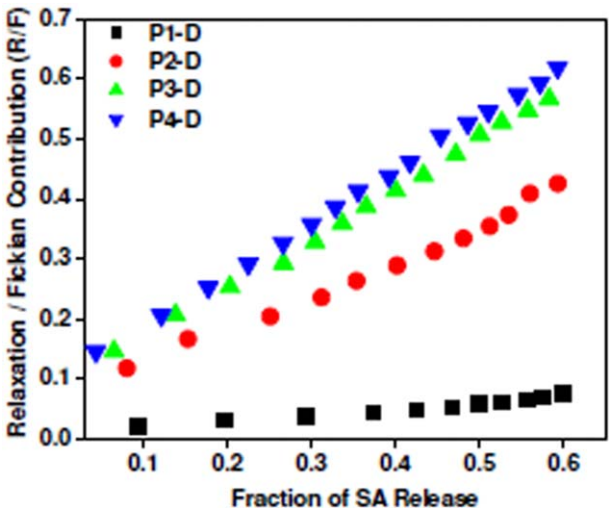

Figure 13. Plot of R/F with the fraction of SA release for the P1-D, P2-D, P3-D, and P4-D hydrogels. [Color figure can be viewed in the online issue, which is available at wileyonlinelibrary.com.]

slowest release of SA and, hence, could be used as a controlled delivery system.

To study the effect of the nature of the drug on the release process, the release of IBF, a relatively hydrophobic drug (molar solubility of IBF at 25°C = 0.552×10^{-4})[57] in comparison to SA (solubility of SA at 25°C ≈ 2.2×10^{-3})[58,59] was monitored from the P4-D and P4C-D hydrogels. Figure 12 shows the release profiles of IBF from the P4-D and P4C-D hydrogels; the release profiles of SA from the same hydrogels were also included for comparison. As expected, a sustained release for IBF was obtained from the P4C-D hydrogel as opposed to the burst release obtained from the P4-D hydrogel; this was similar to that of SA. When the SA and IBF releases were compared from the P4-D hydrogel, there was not much of a difference, but from the P4C-D hydrogel, the release of IBF was prolonged further than that of SA. The difference in the rates of release of IBF and SA could be explained the binding efficiencies of the two drugs with β-CD. The association constant for IBF with β-CD ($K_{IBF-\beta-CD} \approx 10^3\ M^{-1}$) was almost an order higher than that for SA ($K_{SA-\beta-CD} = 119 \pm 6\ M^{-1}$).[60–62] The stronger the binding efficiency between the β-CD and the drug was, the slower the diffusion of drug was from the β-CD. This resulted in a slower release of the drug from the hydrogel matrix. Thus, the nature of the drug in terms of its binding efficiency with the CD played an important role in the drug-delivery process.

Release Kinetics. The fundamental kinetic analyses of the drug-release data revealed the probable release mechanism from the hydrogels. The release data showed the best fit to Ritger–Peppas and Peppas–Sahlin models in all cases (Table IV). The n values were between 0.5 and 1 for all hydrogels, except for P4C-D. The value of n between 0.5 and 1 indicated the anomalous nature of drug release from the hydrogels, where both the diffusion and relaxation processes contribute. From the Peppas–Sahlin equation, we discovered that k_1 dominated over the relaxation kinetic constant (k_2) for the P1-D, P2-D, P3-D, and P4-D hydrogels. It

Table IV. Fitting of the SA and IBF Release Parameters to Various Mathematical Models

	Higuchi		Ritger–Peppas			Peppas–Sahlin			Zero-order	
Sample	k ($h^{-0.5}$)	R^2	n	k' (h^{-n})	R^2	k_1 ($h^{-0.5}$)	k_2 (h^{-1})	R^2	k'' (h^{-1})	R^2
P1-D (SA)	0.358	0.951	0.55	0.347	0.976	0.337	0.014	0.972	0.238	0.631
P2-D (SA)	0.324	0.947	0.62	0.298	0.974	0.242	0.057	0.970	0.217	0.796
P3-D (SA)	0.286	0.957	0.65	0.25	0.992	0.194	0.056	0.988	0.170	0.855
P4-D (SA)	0.218	0.915	0.74	0.149	0.995	0.103	0.052	0.995	0.098	0.933
P1C-D (SA)	0.141	0.953	0.63	0.103	0.982	0.102	0.011	0.978	0.038	0.815
P2C-D (SA)	0.133	0.959	0.64	0.093	0.994	0.091	0.012	0.992	0.036	0.848
P3C-D (SA)	0.102	0.977	0.69	0.077	0.992	0.079	0.005	0.992	0.021	0.815
P4C-D (SA)	0.073	0.818	1.00	0.015	0.994	−0.002	0.015	0.994	0.015	0.994
P4-D (IBF)	0.169	0.891	0.81	0.094	0.995	0.058	0.042	0.997	0.064	0.968
P4C-D (IBF)	0.056	0.796	1.00	0.007	0.994	−0.006	0.01	0.995	0.009	0.992

R^2, fitting parameter.

was not possible to exactly know the contribution of the Fickian or Case II mechanism from the estimated values of k_1 and k_2 alone.[40] Hence, R/F was calculated for the samples and plotted against the fraction of the drug released from these hydrogels (Figure 13). The fractional values of R/F clearly indicated the predominance of diffusion process over the relaxation process, and with the increased GA content, the R/F value also increased.

For a given GA percentage, the value of n was slightly higher for the hydrogels containing the drug–β-CD IC as compared to those containing free drug. For the P1C-D, P2C-D, and P3C-D hydrogels, k_1 dominated over a relaxation kinetic constant (k_2) very similar to those observed for the P1-D, P2-D, P3-D, and P4-D hydrogels. With increasing GA concentration, the R/F value was found to increase. The P4C-D hydrogel, however, showed a case II transport mechanism ($n = 1$) associated with the dominant relaxational release of drug. This was evident from the lower magnitude and negative values of k_1 for both SA and IBF release. This was further supported by the fact that the release data from this film fit quite well with the zero-order kinetics. Thus, the presence of β-CD at a high crosslinker concentration influenced the relaxation rate of the polymer chains and further slowed the release of the drug from the hydrogel matrix. This could be explained by the fact that GA not only crosslinked the PVA chains but also interacted with the hydroxyl groups of β-CDs and thereby influenced the matrix structure.[63]

Thus, from the above studies, it is clear that the role of β-CD in the drug-release process is not only because of its inclusion ability but also its effect on the polymer relaxation. In other words, it is the combined effect of drug diffusion and polymer relaxation that controls the overall drug-release process from the hydrogels containing β-CD.

Cytotoxicity Assay

To test the biocompatibility of the synthesized hydrogels, cytotoxicity assay was performed. As shown in Figure 14, direct contact between the L-929 cells and P4C hydrogel sample did not reveal any adverse effects. No cell death or effects on the cell morphology were observed under the microscope. This suggested a high compatibility of the hydrogels with the living tissues.

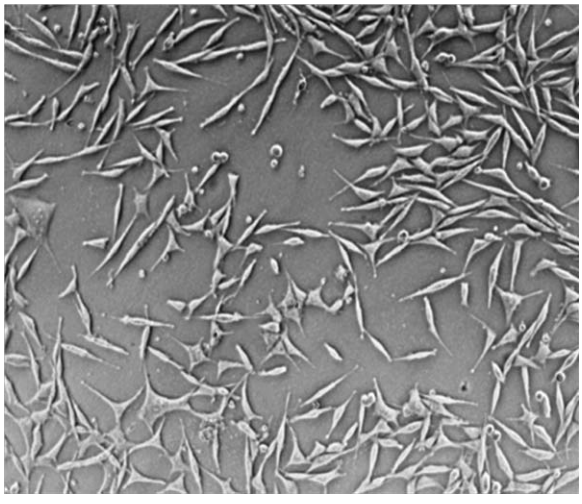

Figure 14. Optical micrographs of L-929 cells cultured after 48 h of incubation with the P4C hydrogel.

CONCLUSIONS

Poly(vinyl alcohol) (PVA) hydrogels were synthesized with various amount of the crosslinker GA. To the hydrogels, preformed drug–β-CD ICs were added. The solid IC of the drug and β-CD was prepared via the coprecipitation method, and this was affirmed by FTIR spectroscopy, XRD, and optical microscopy. The hydrogels were characterized by FTIR spectroscopy, XRD, DSC, and SEM. The swelling evaluation indicated decreased swelling with increasing crosslinker content for both the PVA and the β-CD containing hydrogels. For a given GA concentration, the swellability of the PVA hydrogel was a little higher than that of the β-CD containing hydrogels. The presence of β-CD in the hydrogel resulted in the sustained release of a drug for a prolonged period of time. The preliminary kinetic analysis revealed the anomalous nature of drug release from the P1-D, P2-D, P3-D, P4-D, P1C-D, P2C-D, and P3C-D hydrogels; this indicated the importance of drug diffusion over polymer relaxation. The P4C-D hydrogel, however, showed a case II transport mechanism and indicated the dominant relaxational process. GA, apart from crosslinking PVA, probably interacted with the hydroxyl groups of β-CDs and, thereby, influenced the matrix structure. The rates of release of SA and IBF also varied greatly from the P4C-D hydrogel because of the difference in their binding efficiencies with β-CD. Thus, the drug release was accomplished as a combination of the effects of drug diffusion, hydrogel polymer relaxation, interaction of GA with β-CD, and binding affinity of the drugs with β-CD. The cytotoxicity tests performed on the hydrogels ensured the hydrogels as biocompatible and, hence, could be used as controlled drug-delivery systems.

ACKNOWLEDGMENTS

The authors thank the Department of Science and Technology, India for its financial support.

REFERENCES

1. Wichterle, O.; Lim, D. *Nature* **1960**, *125*, 117.
2. Peppas, N. A.; Mikos, A. G. In Hydrogels in Medicine and Pharmacy; Peppas, N. A., Ed.; CRC: Boca Raton, FL, **1986**; Vol. *1*.
3. Brannon-Peppas, L. In Absorbent Polymer Technology; Brannon-Peppas, L., Harland, R. S., Eds.; Elsevier: Amsterdam, **1990**.
4. Peppas, N. A.; Bures, P.; Leobandung, W.; Ichikawa, H. *Eur. J. Pharm. Biopharm.* **2000**, *50*, 27.
5. Lee, K. Y.; Mooney, D. *J. Chem. Rev.* **2001**, *101*, 1869.
6. Hoare, T. R.; Kohane, D. S. *Polymer* **2008**, *49*, 1993.
7. Tyliszczak, B.; Pielichowski, K. *J. Polym. Res.* **2013**, *20*, 191.
8. Fukutomi, T.; Asakawa, K.; Kihara, N. *Chem. Lett.* **1997**, *8*, 783.
9. Saito, R.; Yoshida, S.; Ishizu, K. *J. Appl. Polym. Sci.* **1997**, *63*, 849.

10. Constantin, M.; Fundueanu, G.; Bortolotti, F.; Cortesi, R.; Ascenzi, P.; Menegatti, E. *Int. J. Pharm.* **2004**, *285*, 87.
11. Kurkuri, M. D.; Aminabhani, T. M. *J. Controlled Release* **2004**, *96*, 9.
12. Sullad, A. G.; Manjeshwar, J. S.; Aminabhavi, T. M. *J. Appl. Polym. Sci.* **2010**, *117*, 1361.
13. Lee, S. G.; Lyoo, W. S. *J. Appl. Polym. Sci.* **2008**, *107*, 1701.
14. Paradossi, G.; Cavalieri, F.; Chiessi, E. *J. Mater. Sci.: Mater. Med.* **2003**, *14*, 687.
15. Cerroni, B.; Chiessi, E.; Margheritelli, S.; Oddo, L.; Parradossi, G. *Biomacromolecules* **2011**, *12*, 593.
16. Lee, M. S.; Mok, E. Y.; Shin, W. C.; Kim, J. D.; Kim, J.-C. *Korean J. Chem. Eng.* **2012**, *29*, 1108.
17. Deshpande, D. S.; Bajpai, R.; Bajpai, A. K. *J. Polym. Res.* **2012**, *19*, 9938.
18. Kobayashi, M.; Hyu, H. S. *Materials* **2010**, *3*, 2753.
19. Gajra, B.; Pandya, S. S.; Vidyasagar, G.; Rabari, H.; Dedania, R. R.; Rao, S. *Int. J. Pharm. Res.* **2012**, *4*, 2.
20. El Malsawi, K. M. *J. Macromol. Sci. Chem.* **2007**, *44*, 541.
21. Bourke, S. L.; Khalili, M. A.; Briggs, T.; Michniak, B. B.; Kohn, J. P. W. *AAPS Pharm. Sci.* **2003**, *5*, 33.
22. Zhao, L.; Mitomo, H.; Zhai, M.; Yoshii, F.; Nagasawa, N.; Kume, T. *Carbohydr. Polym.* **2003**, *53*, 439.
23. Dai, W. S.; Barbari, T. A. *J. Membr. Sci.* **1999**, *156*, 67.
24. Xiao, C.; Zhou, G. *Polym. Degrad. Stab.* **2003**, *81*, 297.
25. Huang, X.; Brazel, C. S. *J. Controlled Release* **2001**, *73*, 121.
26. Bai, H.; Li, C.; Wang, X.; Shi, G. *Chem. Commun.* **2010**, *46*, 2376.
27. Nugent, M. J. D.; Higginbotham, C. L. *Eur. J. Pharm. Biopharm.* **2007**, *67*, 377.
28. Lynch, I.; Gregorio, P.; Dawson, K. A. *J. Phys. Chem. B* **2005**, *109*, 6257.
29. Gulsen, D.; Chauhan, A. *Int. J. Pharm.* **2005**, *292*, 95.
30. Kanjickal, D.; Lopina, S.; Evancho-Chapman, M. M.; Schmidt, S.; Donovan, D. *J. Biomed. Mater. Res. A* **2005**, *74*, 454.
31. Siemoneit, U.; Schmitt, C.; Alvarez-Lorenzo, C.; Luzardo, A.; Otero-Espinar, F.; Concheiro, A. *Int. J. Pharm.* **2006**, *312*, 66.
32. Sreenivasan, K. *J. Appl. Polym. Sci.* **1997**, *65*, 1829.
33. Sun, P.; Chen, J.; Liu, Z.-W.; Liu, Z.-T. *J. Macromol. Sci. Pure Appl. Chem.* **2009**, *46*, 533.
34. Bazhban, M.; Nouri, M.; Mokhtari, J. *Chin J. Polym. Sci.* **2013**, *31*, 1343.
35. Xu, J.; Li, X.; Sun, F.; Cao, P. *J. Biomater. Sci. Polym. Ed.* **2010**, *21*, 1023.
36. Yamamoto, Y.; Tagawa, S. *Radiat. Phys. Chem.* **2004**, *69*, 347.
37. Salústio, P. J.; Feio, G.; Figueirinhas, J. L.; Pinto, J. F.; Cabral Marques, H. M. *Eur. J. Pharm. Biopharm.* **2009**, *71*, 377.
38. Higuchi, T. *J. Pharm. Sci.* **1963**, *52*, 1145.
39. Ritger, P. L.; Peppas, N. A. *J. Controlled Release* **1987**, *5*, 37.
40. Peppas, N. A.; Sahlin, J. *J. Int. J. Pharm.* **1989**, *57*, 169.
41. Maoa, S.; Shuaia, X.; Ungera, F.; Wittmara, M.; Xiec, X.; Kissela, T. *Biomaterials* **2005**, *26*, 6343.
42. Phan, T. N. T.; Bacquet, M.; Laureyns, J.; Morcellet, M. *Phys. Chem. Chem. Phys.* **1999**, *1*, 5189.
43. Gao, Z. W.; Zhao, X. P. *J. Colloid Interface Sci.* **2005**, *289*, 56.
44. Belyakova, L. A.; Varvarin, A. M.; Lyashenko, D. Y.; Khora, O. V.; Oranskaya, E. I. *Colloid J.* **2007**, *69*, 546.
45. Mura, P.; Bettinetti, G. P.; Manderioli, A.; Faucci, M. T.; Bramanti, G.; Sorrenti, A. *Int. J. Pharm.* **1998**, *166*, 189.
46. Hussein, K.; Turk, M.; Wahl, M. A. *Pharm. Res.* **2007**, *24*, 585.
47. Froemming, K. H.; Szejtli, J. Cyclodextrins in Pharmacy; Kluwer: Dordrecht, The Netherlands, **1994**.
48. Harata, K. *Chem. Rev.* **1998**, *98*, 1803.
49. Fernandes, C. M.; Vieira, M. T.; Veiga, F. J. B. *Eur. J. Pharm. Sci.* **2002**, *15*, 79.
50. Rotich, M. K.; Brown, M. E.; Glass, B. D. *J. Therm. Anal. Calorim.* **2003**, *73*, 671.
51. Greatbanks, D.; Pickford, R. *Magn. Reson. Chem.* **1987**, *25*, 208.
52. Hari, P. R.; Sreenivasan, K. *J. Appl. Polym. Sci.* **2001**, *82*, 143.
53. Figueiredo, K. C. S.; Alves, T. L. M.; Borges, C. P. *J. Appl. Polym. Sci.* **2009**, *111*, 3074.
54. Peppas, N. A.; Merrill, E. W. *J. Appl. Polym. Sci.* **1976**, *20*, 1457.
55. Hassan, C. M.; Peppas, N. A. *Adv. Polym. Sci.* **2000**, *153*, 37.
56. Mansur, H. S.; Sadahira, C. M.; Souza, A. N.; Mansur, A. A. P. *Mater. Sci. Eng. C* **2008**, *28*, 539.
57. Garzon, L. C.; Martinez, F. *J. Solution Chem.* **2004**, 33.
58. Shalmashi, A.; Eliassi, A. *J. Chem. Eng. Data* **2008**, *53*, 199.
59. Pires, R. F.; Franco, M. R., Jr. *Fluid Phase Equilib.* **2012**, *330*, 48.
60. Belyakova, L. A.; Lyashenko, D. Y. *J. Appl. Spectrosc.* **2008**, *75*, 299.
61. Hergert, L. A.; Escandar, G. M. *Talanta* **2003**, *60*, 235.
62. Manzoori, J. L.; Amjadi, M. *Spectrochim. Acta A* **2003**, *59*, 909.
63. Bibby, D. C.; Davies, N. M.; Tucker, I. G. *Int. J. Pharm.* **2000**, *197*, 1.